

Defective Kernel 39 encodes a PPR protein required for seed development in maize^{oo}

Xiaojie Li[†], Wei Gu[†], Silong Sun, Zongliang Chen, Jing Chen, Weibin Song, Haiming Zhao and Jinsheng Lai^{*}

State Key Laboratory of Agrobiotechnology and National Maize Improvement Center, Department of Plant Genetics and Breeding, China Agricultural University, Beijing 100193, China

[†]These authors contributed equally to this work.

*Correspondence: Jinsheng Lai (jlai@cau.edu.cn)

doi: 10.1111/jipb.12602

Abstract RNA editing is a posttranscriptional process that is important in mitochondria and plastids of higher plants. All RNA editing-specific trans-factors reported so far belong to PLS-class of pentatricopeptide repeat (PPR) proteins. Here, we report the map-based cloning and molecular characterization of a defective kernel mutant *dek39* in maize. Loss of *Dek39* function leads to delayed embryogenesis and endosperm development, reduced kernel size, and seedling lethality. *Dek39* encodes an E sub-class PPR protein that targets to both mitochondria and chloroplasts, and is involved in RNA editing in mitochondrial NADH dehydrogenase3 (*nad3*) at *nad3-247* and *nad3-275*. C-to-U editing of *nad3-275* is not conserved and even lost in *Arabidopsis*, consistent with the idea that no close

DEK39 homologs are present in *Arabidopsis*. However, the amino acids generated by editing *nad3-247* and *nad3-275* are highly conserved in many other plant species, and the reductions of editing at these two sites decrease the activity of mitochondria NADH dehydrogenase complex I, indicating that the alteration of amino acid sequence is necessary for Nad3 function. Our results indicate that *Dek39* encodes an E sub-class PPR protein that is involved in RNA editing of multiple sites and is necessary for seed development of maize.

Edited by: Jianping Hu, Michigan State University, USA

Received Jul. 30, 2017; **Accepted** Sept. 30, 2017; **Online on** Oct. 5, 2017

OO: OnlineOpen

Research Article

OnlineOpen

INTRODUCTION

The pentatricopeptide repeat (PPR) protein family is one of the largest families in the angiosperms (Barkan and Small 2014), with 450 members in *Arabidopsis thaliana* and 477 in rice (O'Toole et al. 2008). Typically, PPR proteins contain 2 to 26 tandemly repeated PPR motifs (Lurin et al. 2004). PPR proteins have been divided into two subclasses (P-PPR and PLS-PPR): the P-PPR proteins consist of a tandem alignment of canonical 35-amino-acid PPR motifs (P-motif), and the PLS-PPR proteins, which are characterized by additional longer and shorter PPR motifs, form tandemly repeated triplets, P-L-S (Lurin et al. 2004; Schmitz-Linneweber and Small 2008). PLS-PPR proteins mostly possess additional C-terminal domains, E (extension) or DYW

domain, which further classified the PLS-class into E and DYW sub-class.

Most PPR proteins localize in mitochondria or chloroplasts, or both organelles, where they bind RNA in a sequence-specific manner and function in a number of aspects, including RNA stability, RNA splicing, translation and RNA editing. RNA editing is a posttranscriptional mechanism that alters, inserts or deletes nucleotides in RNA molecules so that the genetic information in mature RNA differs from the prediction of the genomic DNA. In flowering plants, RNA editing is performed generally as a deamination of specific cytidines (C) so that the nucleotide C changes to uridine (U). RNA editing is frequently observed in mitochondria and chloroplasts (Takenaka et al. 2013; Shikanai 2015). The C-to-U RNA editing events play important roles in gene expression,

© 2017 The Authors. *Journal of Integrative Plant Biology* Published by John Wiley & Sons Australia, Ltd on behalf of Institute of Botany, Chinese Academy of Sciences

This is an open access article under the terms of the Creative Commons Attribution-NonCommercial License, which permits use, distribution and reproduction in any medium, provided the original work is properly cited and is not used for commercial purposes.

including generating initiation codons by changing ACG to AUG (Hoch et al. 1991; Hirose and Sugiura 1997), correcting codons to encode conserved amino acids (Maier et al. 1992) and introducing translation termination by generating required stop codons (Wakasugi et al. 1996).

C-to-U editing is not highly conserved in all land plants. In the *Marchantia* clade of the liverworts, editing has been reported to be completely lost (Takenaka et al. 2013). Even between closely related species or different ecotypes of the same species, differences in whether RNA editing occurred in individual sites are detected. Seven RNA editing sites with 40%–60% differences in effective editing between Col, Ler, and C24 ecotypes of *Arabidopsis* were reported (Zehrmann et al. 2008). On the other hand, in maize and *Petunia*, incompletely edited mitochondrial mRNAs are prevalent (Grosskopf and Mulligan 1996; Wilson and Hanson 1996). The frequency of editing at some sites differs among tissues and developmental stages (Grosskopf and Mulligan 1996; Hirose and Sugiura 1997), indicating that RNA editing can be highly variable.

Subsequent to the identification of *Arabidopsis* CRR4 for an RNA editing event in chloroplasts (Kotera et al. 2005), more and more PPR proteins have been discovered as trans-factors. So far, all RNA-editing specificity-factors identified are members of PLS-class PPR (Barkan and Small 2014). PLS-PPR proteins recognize and bind RNA substrates through their PPR motifs, in a sequence-specific manner; the amino acid code used by these PPR proteins for RNA recognition has been reported (Barkan et al. 2012). In *Arabidopsis*, 44 editing sites in the chloroplasts (Ruwe et al. 2013) and 619 sites in the mitochondria (Bentolila et al. 2013) have been identified. These sites are edited by approximately 200 members of the PLS-class family, suggesting that a single trans-factor manages more than two sites, on average. CRR22 (Okuda et al. 2009) and MEF1 (Zehrmann et al. 2009) are involved in at least three sites in plastids and three sites in mitochondria, respectively. PPR2263, EMP9, DEK10 are also trans-factors required in multiple sites editing (Sosso et al. 2012; Qi et al. 2017a; Yang et al. 2017). PPR proteins such as SLG1, SMK1 and EMP7 have been reported to be responsible for single editing sites as well (Yuan and Liu 2012; Li et al. 2014; Sun et al. 2015). In addition, the RNA editing sites are flexible and non-conservative, the respective specificity-conferring PPR proteins may be lost or remain from the nuclear genome because of their requirement for editing of other targeting sites (Takenaka et al. 2013). MEF10 is involved in editing

at *nad2*-842 in *Arabidopsis*, but the site has already changed to T in the grape mitochondria genome. Therefore, the MEF10 ortholog in grape shows low similarity with AtMEF10 (Hartel et al. 2013).

RNA editing appears to be an essential process in plant growth and development, and some loss-of-function mutants exhibit severe defects in embryo and seedling development. PPR2263 encodes a DYW domain-containing PPR protein and is responsible for RNA editing in mitochondria at the *nad5*-1550 and *cob*-908 sites in maize. The *ppr2263* mutant in mitochondria lacks complex III and causes growth defects in kernels and seedlings (Sosso et al. 2012). Another DYW sub-group PPR protein EMP5 is required for RNA editing in mitochondria at the *rpl16*-458 site and nine other sites in *nad9*, *cox3* and *rps12*. Null mutation of *Emp5* blocks the development of both the embryo and the endosperm (Liu et al. 2013). Loss of function in E sub-group PPR protein SMK1 results in the abolishment of the C-to-U RNA editing at *nad7*-836 in both maize and rice, leading to dramatically reduced complex I assembly and embryo and seedling lethality (Li et al. 2014). A lack of editing of *ccmF_N*-1553 in mutant *emp7* leads to the arrest of maize embryogenesis and embryo lethality (Sun et al. 2015).

For PPR proteins localized in mitochondria, defects in embryo and seed development are likely caused by the disruption of the respiratory chain; electrons mainly enter into the chain from NADH through mitochondrial complex I (Hirst 2013). Complex I, a proton-pumping NADH, ubiquinone oxidoreductase, is the largest protein segment that operates in oxidative phosphorylation. Plant mitochondrial complex I is composed of more than 40 subunits, nine of which are encoded by *nad* genes, including *nad3* (Heazlewood et al. 2003). Abolishment of RNA editing at *nad3*-250 in *slg1* resulted in strongly impaired NADH activity of complex I (Yuan and Liu 2012). Reduction of editing efficiency at *nad3*-61, *nad3*-62 and *cox2*-550 in *dek10* resulted in the decrease of Nad3 and COX2 protein accumulation, which further led to the activity defect in complex I and complex IV (Qi et al. 2017a). Therefore, correcting codons to encode conserved amino acids of Nad3 is essential for maintaining high activity of complex I.

In this study, we report the cloning and molecular characterization of a nuclear gene *Dek39*, which affects embryo and endosperm development and seedling growth in maize. Map-based cloning identified a point

mutation in *Dek39* responsible for the mutant phenotype. *Dek39* encodes an E sub-group PPR protein that dually targets to mitochondria and plastids. Functional analysis indicated that DEK39 is involved in RNA editing at *nad3*-247 and *nad3*-275. Therefore, it is important to the proper function of Nad3 in mitochondria NADH dehydrogenase complex I.

RESULTS

Phenotypic and genetic characterization of mutant *dek39*

The defective kernel mutant *dek39* was isolated from a B73 Ethylmethane sulfonate (EMS) mutagenesis population and more than three consecutive

backcrosses were performed on the B73 inbred line to clear up irrelevant mutations. The *dek39* mutant behaved as monogenic recessive traits since the self-pollinated *dek39* heterozygous plant segregated one quarter of the defective kernels (Figure 1A, wild-type: defective kernel, 659:211, $P > 0.95$).

Mature seeds of the *dek39* mutant showed flatter appearance and relatively smaller size in endosperms and embryos compared to their wild-type siblings (Figure 1B). A germination test showed that approximately 80% of the mutant kernels failed to germinate and less than 20% had an emerged primary root and shoot (Figure 1C). In contrast to the wild-type siblings, the *dek39* mutant seedlings exhibited slow growth; meanwhile, the leaves turned yellowish and stunted 7 d

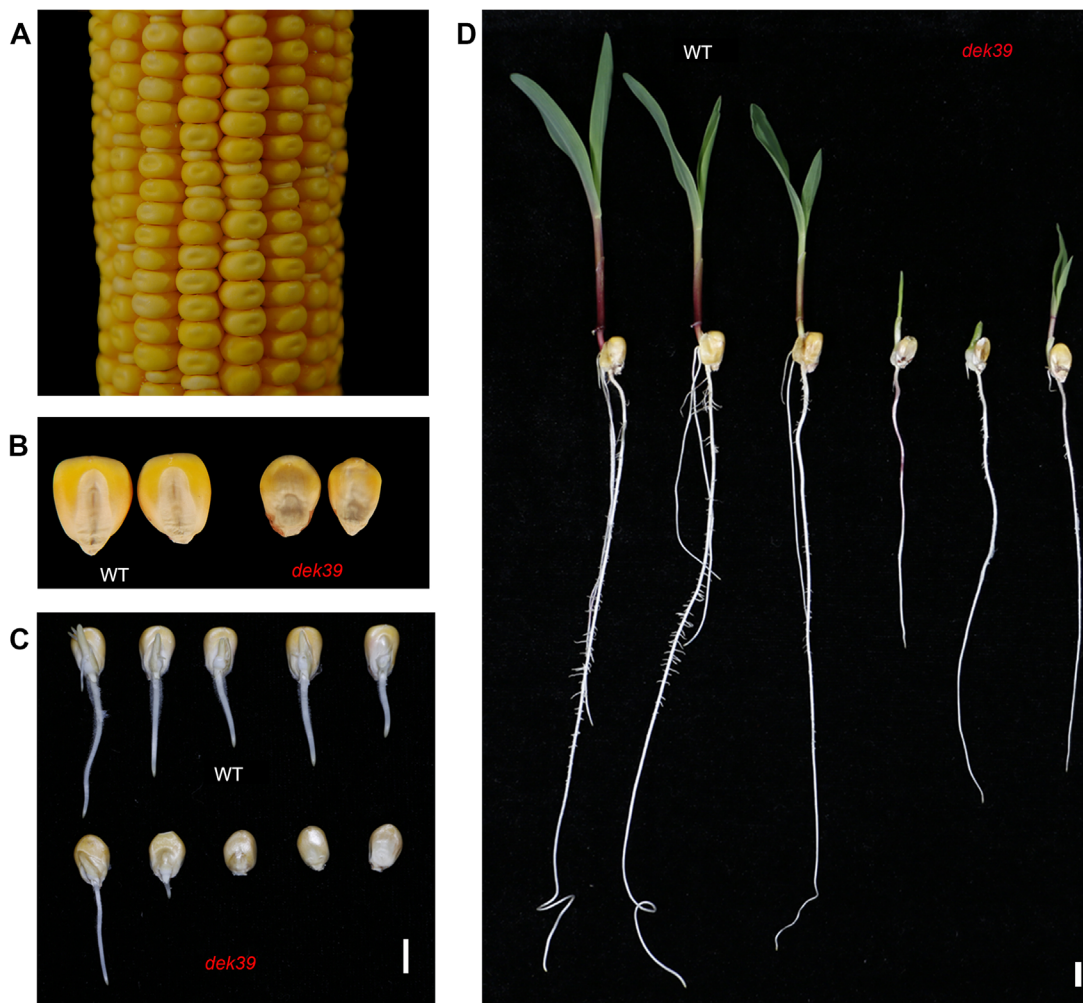


Figure 1. Kernel and seedling phenotype of *dek39*

(A) A mature ear of self-pollinated heterozygous plant segregated for wild-type and miniature kernels. WT, wild-type. (B) Front view of wild-type and *dek39* kernels. (C) Germination test of *dek39* and wild-type siblings. Bar = 1 cm. (D) *dek39* seedlings were short and stunted compared with wild-type at 7 d after germination. Bar = 1 cm.

after sowing (Figure 1D), and eventually these plants died three weeks after germination.

***dek39* showed developmental delay in embryo and endosperm**

The *dek39* kernels not only appeared smaller than normal sibling kernels, but also exhibited a developmental delay.

Cytological sections of *dek39* seeds at 12 DAP (day after pollination) revealed that the mutant embryos had developed into the coleoptilar stage, which is characterized by the formation of the shoot apical meristem (SAM) and root apical meristem (RAM), and the separation of a small protuberance that marks the position of the future coleoptile (Figure 2A). The

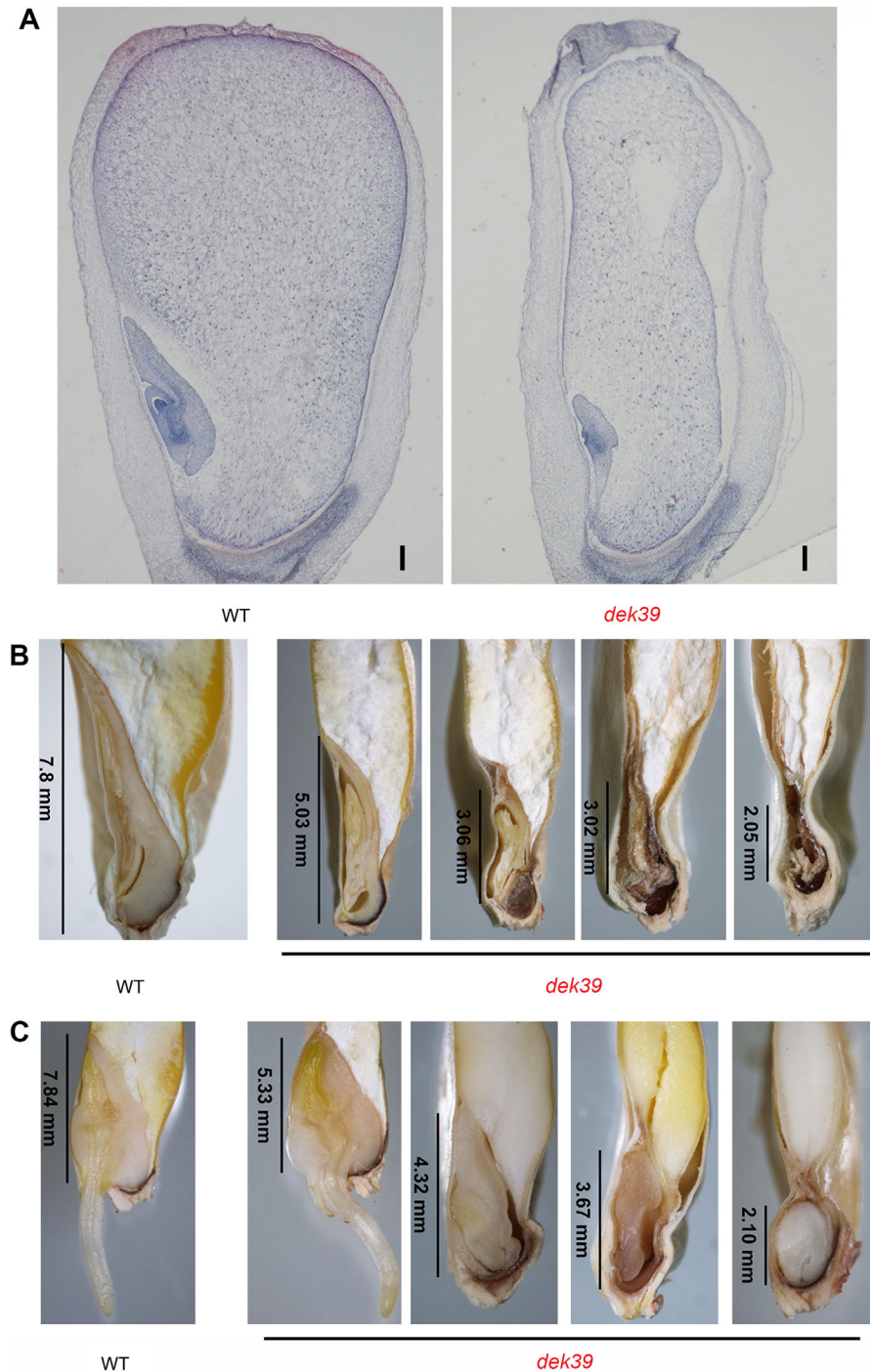


Figure 2. Continued.

endosperm development was disrupted, leaving a gap between the endosperm and the pericarp. By contrast, wild-type embryos at 12 DAP already had differentiated scutellum, two leaf primordia, root apical meristem and visible vascular tissue, and the endosperm was also larger than in the mutant.

At maturity, the average volume of *dek39* mutant endosperms represented approximately one-third that of the wild-type sibling endosperms. Nevertheless, *dek39* embryos showed variable severity, ranging from being normal to nearly empty (Figure 2B). Almost 80% of *dek39* kernels with severe defects in embryogenesis failed to germinate (Figure 2C), and all *dek39* seedlings died three weeks after germination. These lethal phenotypes suggested that *dek39* is indeed involved in multiple developmental stages in maize.

Map-based cloning of *Dek39*

To identify the causative gene for *dek39* phenotype, we performed map-based cloning (Xia et al. 2006). The mapping population was collected from an F₂ generation obtained from crossing the heterozygous *dek39* mutants with Mo17. As a first step, we determined the genetic linkage of mutation site to three markers on chromosome 9 (9–50.1 Mb, 9–96.5 Mb, 9–149.7 Mb) (Figure 3A). Additional markers were used to narrow down the mutation region, and finally, the mutation was mapped between 9–111.3 Mb and 9–112.5 Mb. According to MaizeGDB, there were 13 predicted genes in this region, so we designed PCR primer pairs to amplify all of these genes from mutant *dek39*, which were later sequenced and assembled. Compared with sequences of these genes amplified from the wild-type, we identified a G-to-A alteration in gene GRMZM2G345128, which resulted in Trp being converted to a stop codon (Figure 4A).

The entire length of GRMZM2G345128 was not available because there was a gap, 1,205 bp downstream from the predicted start codon on RefGen_V2 in

this gene. Total RNAs extracted from B73 kernels (12 DAP) were used for full-length GRMZM2G345128 cDNA synthesis, according to the rapid amplification of cDNA ends (RACE) protocol. The *Dek39* cDNA consisted of a 1,252-bp-long 5'UTR, a 2,286-bp-long ORF, and a 249-bp-long 3' UTR. Genomic DNA sequence of this gene was generated using gene-specific primers corresponding to a full-length cDNA. Alignment of the two sequences revealed that *Dek39* contained a single exon. The mutation was located at 201 bp downstream from the start codon, and resulted in a premature stop codon.

Complementation of the *dek39* mutation through genetic transformation

To confirm that GRMZM2G345128 is the causative gene for *Dek39*, we performed complementation of the *dek39* with a GRMZM2G345128 transgenic construct. The GRMZM2G345128 promoter along with the entire coding sequence was amplified from genomic DNA and fused with a MYC tag at the C-terminus on the vector pCAMBIA3100. Since the mutant *dek39* was lethal, we introduced the construct into the B73 inbred line, and then crossed the transgenic plants with heterozygous (+/*dek39*) plants. Segregating ears of self-pollinated double heterozygous (+/*dek39*, –/*Dek39*-MYC) plants showed that the frequency of small kernels was (5.5% ± 1.2%) much closer to the 1:16 ratio expected rather than the 1:4 ratio (Figure 3B). Southern blotting was performed to analyze the integration of the transgene and confirm its presence in complemented transgenic lines (Figure 3C).

In order to verify whether the construct could recover the seedling lethality of *dek39*, we chose kernels that carried the construct, and were homozygous for the mutation, to analyze germination and seedling phenotype. All chosen kernels exhibited normal germination ratio and similar seedling growth phenotypes as the wild-type (Figure 3D). These results showed that both kernel phenotype and plant phenotype could be

Figure 2. *dek39* exhibited development delay in both endosperm and embryo
 (A) Developmental comparisons of wild-type (WT; left) and *dek39* kernel (right) at 12 days after pollination (DAP). The endosperm development of *dek39* was obviously delayed, leaving a gap between endosperm and pericarp. The *dek39* embryo reached coleoptile stage while wild-type embryo had developed leaf primordial and root apical meristem. Bar = 1 mm. (B, C) Dissection of mature and germinated wild-type (WT; left) and *dek39* (right) kernels. In comparison to wild-type siblings, *dek39* embryos showed variable severity, ranging from almost normal differentiated to nearly empty embryo.

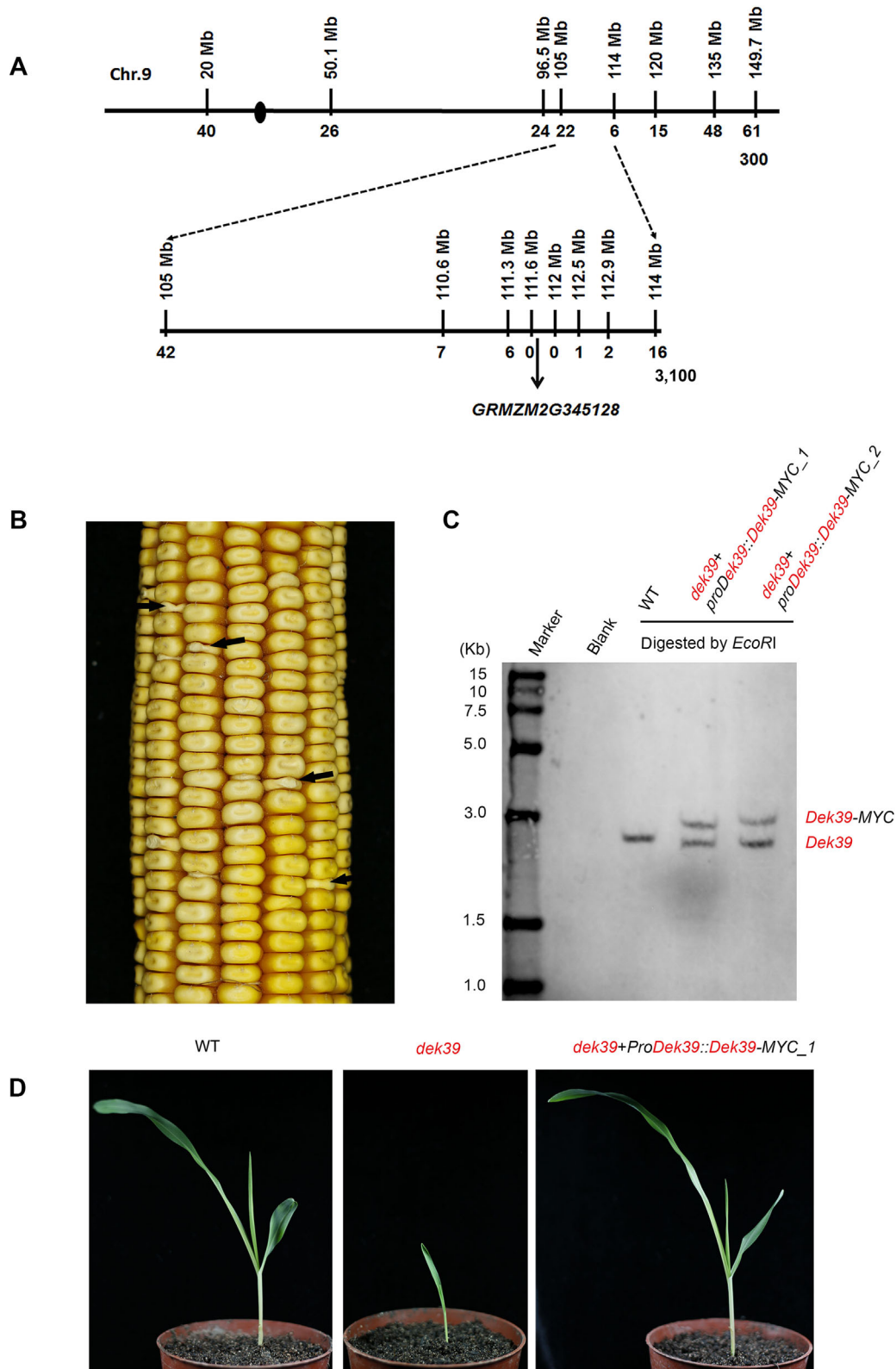


Figure 3. Map based cloning of *dek39* and complementation of the *dek39* mutation with genetic transformation
(A) At first-pass mapping, 300 individual miniature kernels were genotyped and genetic linkage to three markers (9–50.1 Mb, 9–96.5 Mb, 9–149.7 Mb) on chromosome 9 was identified. Additional markers were detected to narrow down the mutation region between markers 9–105 Mb and 9–114 Mb. A population of 3,100 small kernel samples

complemented by *ProDek39::Dek39-MYC*, which provided evidence that the mutation in gene *Dek39* indeed led to the observed *dek39* phenotypes.

Dek39 encodes a PPR protein of the E subfamily

BLAST analysis of the deduced amino acid sequence of *Dek39* revealed high similarity to the conserved domains of pfam01535, which classified the encoded protein as a member of the PPR superfamily. More detailed motif prediction analysis in PLANTPPR (<http://www.plantppr.com>) (Cheng et al. 2016) revealed that DEK39 contained canonical (P), long (L), and short (S) PPR motifs forming repeated P-L-S triplets (Figure 4B). The PLS triplets were not in consecutive order but were interrupted by several short PPR motifs. Successive additions of E (extension) domains were identified at the C-terminus. Therefore, DEK39 is a PPR-E protein (Lurin et al. 2004; Barkan and Small 2014). The lack of similarity between the amino acid sequences of maize and *Arabidopsis* showed that there were no DEK39 homologs in *Arabidopsis*. However, DEK39 has a closely related rice homolog Os06g0143500 with 70% identity (Figure S1).

In the mutant *dek39*, the premature stop codon within the coding sequence led to a deletion of almost the entire DEK39 protein, leaving only 67 amino acids, including the mitochondrial signaling peptide and the first PPR motif (Figure 4B).

Ubiquitous expression of Dek39

Since there were no expressed sequence tags corresponding to *Dek39* available in the database, we searched published RNA-seq data to find expression information (Chen et al. 2014). The RNA-seq reads could cover the full-length *Dek39* cDNA sequence, confirming the gene model of *Dek39* obtained from our RACE results.

We next performed quantitative RT-PCR with gene-specific primers to provide experimental evidence for

Dek39 expression patterns in major maize tissues and developing kernels. *Dek39* was expressed in all vegetative and reproductive maize tissues tested (Figure 4C). Relatively high expression was observed in the ear, with intermediate expression in early (6 DAP, 8 DAP) and later (32 DAP) stages of kernel development, with the weakest expression in the root, stem, leaf, tassel and developing kernel, between 10 and 24 DAP. Ubiquitous expression pattern of *Dek39* indicated *Dek39* may have functions throughout all stages of plant growth and development.

Dual localization of DEK39 in mitochondria and chloroplasts

PPR superfamily proteins are mostly targeted to organelles and the dual targeting to mitochondria and chloroplasts occurs more frequently than expected. Sequence analysis of DEK39 with the TargetP algorithm (Emanuelsson et al. 2000) (<http://www.cbs.dtu.dk/services/TargetP/>) predicted the dual localization trait of DEK39 to both of these organelles. The probability for localization in mitochondria (0.66) was higher than that in chloroplasts (0.34).

To experimentally determine the subcellular localization of DEK39, a translation fusion of full-length *Dek39* with green fluorescent protein (GFP) was generated under the control of a 35S promoter and applied to a transient expression analysis, via infiltrating *Nicotiana benthamiana* leaves with *Agrobacterium tumefaciens*. Here, the green fluorescent signal was either absent or low. Similarly, it was reported that the signal of full-length EMP5 fused to GFP could not be detected due to the size of the fusion protein (Liu et al. 2013). So instead, we substituted the full-length DEK39 with the N terminal 417 amino acids of DEK39, which contains 12 PPR motifs, leaving other conditions unchanged. The translation fusion construct *Dek39*^{N417}-GFP was transiently expressed in epidermal cells of tobacco leaves, and the fluorescent signal was detected by confocal laser scanning microscopy. Red auto-fluorescent (chloroplast)

was used for fine mapping and additional six markers were detected to narrow down the mutation region. Finally, an interval of 1.3 Mb containing mutation was determined and all predicted genes in this region were sequenced. Comparison with B73 identified a mutation G to A in GRMZM2G345128. (B) Ear of self-pollinated the double heterozygotes (+/*dek39*; transgene *Dek39*/-) plant showed the frequency of small kernels was (5.5% ± 1.2%) much closer to the 1:16 ratio expected in the case of complementation than to the 1:4 ratio expected otherwise. Black arrows indicated the phenotype of *dek39*. (C) Analysis of *Dek39-MYC* integration in complemented *dek39* plants by Southern blotting. The transgene seedling showed similar growth phenotype as wild-type (left).

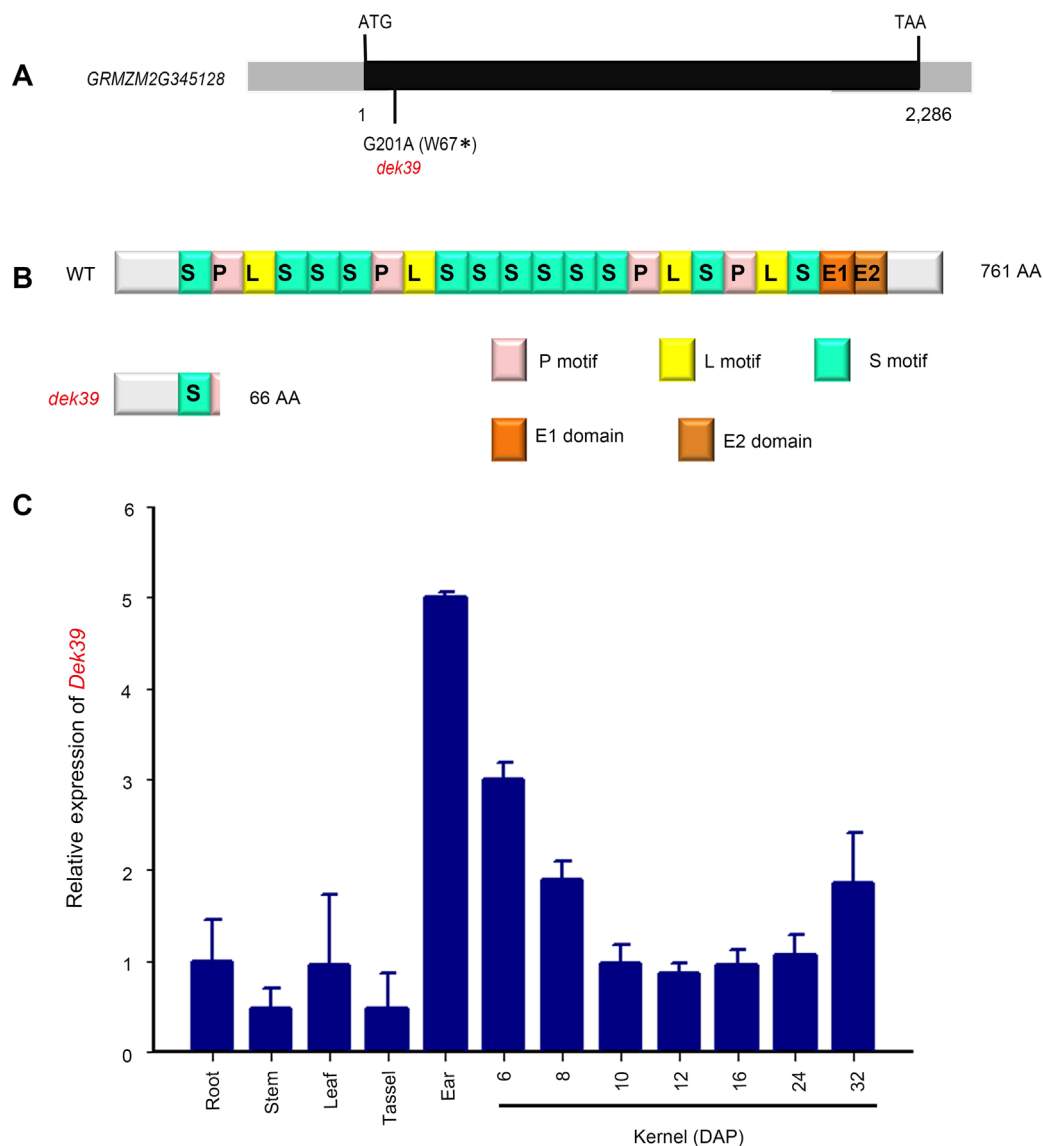


Figure 4. Gene structure and molecular characterization of Dek39 and expression pattern of Dek39

(A) Schematic drawing of the intronless gene *Dek39* and the location of the mutation of *dek39*. (B) Schematic diagram of DEK39 protein. The mutant DEK39 protein was terminated in the first P motif. (C) Quantitative RT-PCR analysis indicated *Dek39* was a ubiquitously expressed gene. Primers Dek39-RT-F and Dek39-RT-R were used in RT-PCR, and EF1a was used as reference gene. qRT-PCR values for *Dek39* were means of three technical replicates. Error bars represented the SD.

and MitoTracker (mitochondria) signals were collected at wavelengths from 650 to 800 nm and from 560 to 650 nm, respectively. The result showed co-localization of the green fluorescent signal of DEK39^{N417}-GFP with both the red auto-fluorescent signal of chloroplasts (Figure 5A–C) and the small red fluorescent dots of mitochondria (Figure 5A–E). By contrast, the green fluorescent signal of the GFP control could be detected throughout the epidermal cells of tobacco leaves (Figure

5B). Together these results indicated that DEK39 is targeted to both mitochondria and chloroplasts.

DEK39 is required for mitochondria RNA editing

To investigate the function of DEK39 in RNA posttranscriptional processing, we compared the mitochondrial and plastid transcript profiles of endosperms in the wild-type and *dek39*. Total RNA was extracted from endosperm at 12 DAP, and ribosomal RNA was removed. The libraries were

constructed without poly-A selection and each sample had two biological replicates. By performing a data saturation analysis, we determined that the number of genes tended to be invariable, suggesting that all CDS in mitochondria

were covered and the data volume was suitable for the following analysis (Figure S2). The two replicates of the transcripts in *dek39* and the wild-type were highly correlated (Figure S3).

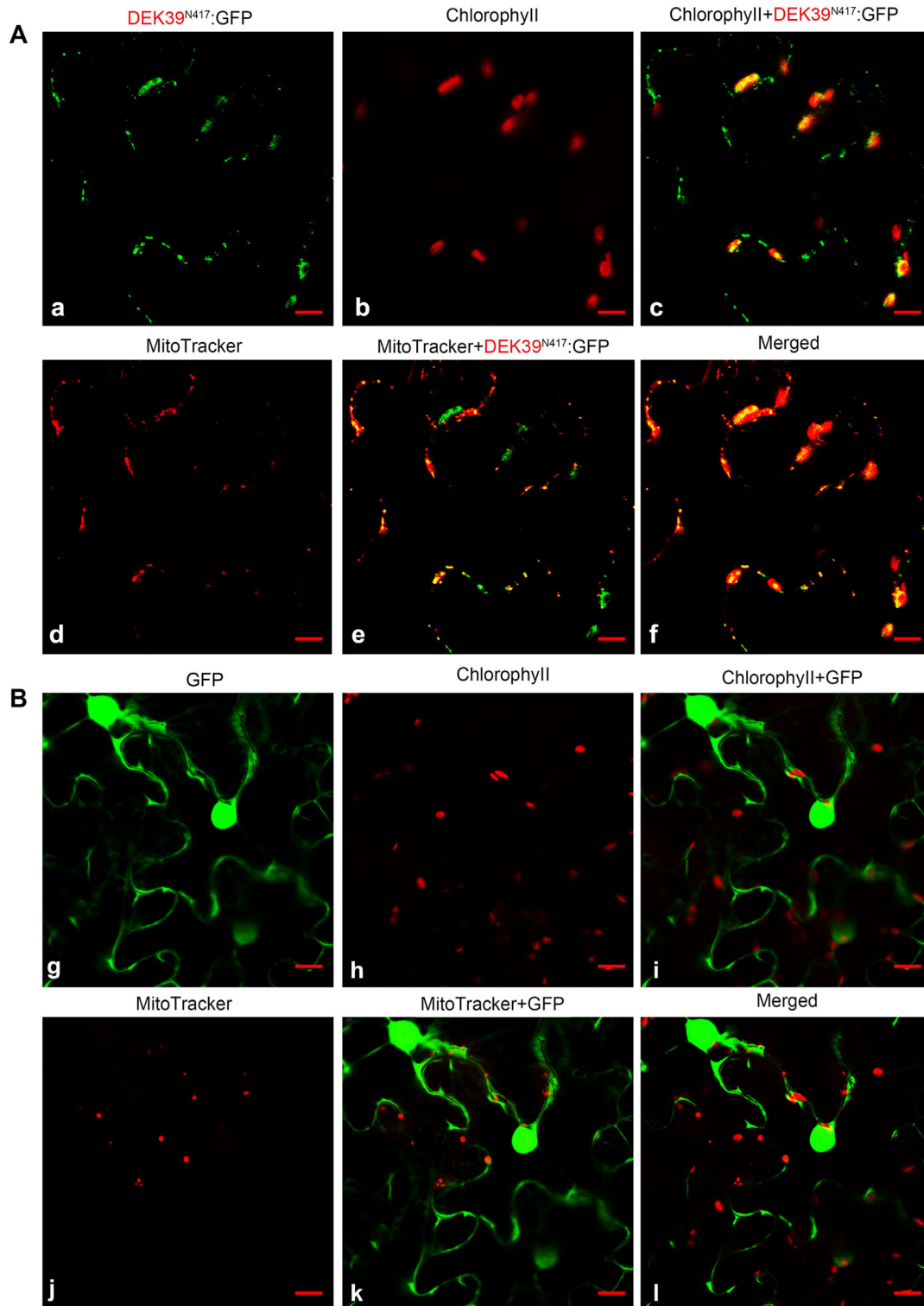


Figure 5. Continued.

To call the RNA editing sites, each sample of the raw reads of the two biological replicates was aligned to the B73 RefGen_V4 Mitochondrial genome of Maize. The coverage of transcripts by the reads was 97.6% and 96.6% in *dek39* and the wild-type, respectively (Table S2). All sites with C-to-U changes in wild-type mitochondrial transcriptome compared with the original DNA sequence were called out. Sites covering more than 10 reads were used for analyzing the editing efficiencies, and 347 sites in mitochondria were detected to be covered by the reads in CDS (Table S4). The sites located within the gene coding region were chosen to analyze the change of editing efficiencies. Editing frequencies of two sites were detected as being significantly decreased (frequency change >20%, and $P < 0.05$) in *dek39*. Editing efficiency of *nad3-247* in *dek39* was 40%, compared with 80% in the wild-type. RNA editing at *nad3-275* was almost lost (4.4% on average) in *dek39*, but 64% of C were edited to U in wild-type.

To confirm these results, mitochondrial cDNA was amplified using *nad3*-specific primers and the PCR products were cloned into pMD-18. Individual clones were sequenced and the results showed that the percentages of C edited to U at *nad3-247* were 68.4% and 68.2% in the wild-type and complemented transgene lines (*dek39 + ProDek39::Dek39-MYC*), respectively, whereas the editing frequency was reduced to 50.7% in *dek39*. RNA editing was not detected in *dek39* at *nad3-275*, but was detected to be edited to 59.6% and 60.3% in the wild-type and complemented transgene lines (Figure 6A). Statistical analysis showed that the differences between the wild-type and complemented transgene lines were not significant at neither *nad3-247* nor *nad3-275*, indicating that *ProDek39::Dek39-MYC* did complement the function of *dek39*.

In flowering plants, *nad3-247* is a conserved editing site, whereas *nad3-275* is not. In *Arabidopsis* and *Brassica*, editing at *nad3-275* has already been lost by its conversion to T in the mitochondrial genome (Figure 6B). RNA editing at *nad3-247* leads to the

presence of a Pro rather than a Ser residue, and editing at *nad3-275* caused the residue to convert from Ser to Phe. An alignment of amino acid sequences from genomic DNA sequences of 13 plant species showed that the two editing events took place in both monocotyledonous and dicotyledonous plants (Figure 6B, C). In the green alga *Chara vulgaris* and the liverwort *Marchantia polymorpha*, no editing sites have been detected (Takenaka et al. 2013). In these two species, Ser and Phe were encoded at *nad3-247* and *nad3-275*, respectively. Editing of *nad3-247* and *nad3-275*, both of which led to amino acid conversions, were reported in monocotyledonous plants *Allium cepa*, *Triticum aestivum*, and dicotyledonous plants *Magnolia grandiflora* (Perrotta et al. 1996; Pesole et al. 1996). For other species, RNA editing information was acquired from the RNA Editing Database (Picardi et al. 2007). Together, the results indicated that the amino acid replacements are necessary for Nad3's function.

To test if DEK39 functioned in plastids, we compared the plastid transcript profiles of the wild-type and *dek39* using RNA-sequencing. Transcript coverage by the reads was 95.9% and 99.2% in *dek39* and the wild-type, respectively (Table S3). Based on information in the Maize B73 RefGen_V4 plastids genome, we detected 24 RNA editing sites, but all of these editing sites in *dek39* were found to be the same as that in the wild-type (Table S5). These results suggested that DEK39 was not involved in RNA editing of plastids.

RNA splicing (Yap et al. 2015b) and RNA stability (Hammani et al. 2016) could be affected in some PLS-PPR mutants, so we next tested the RNA splicing efficiency and the abundance of transcripts of these two organelles in *dek39* using RNA sequencing data. The results showed that there were no differences in RNA splicing between *dek39* and the wild-type in neither mitochondria nor plastids. In addition, no significant differentially expressed genes were identified, indicating that the stability of RNA in these two organelles was not affected in *dek39*.

Figure 5. Subcellular localization of DEK39

(A) DEK39^{N417}:GFP fusion protein that carried the N-terminal 417 amino acids of DEK39 fused with GFP, was transiently expressed in tobacco epidermal cells. (B) GFP protein was used as a control. The red auto-fluorescent signal of chloroplasts and the red fluorescent of Mitochondria marked by MitoTracker were collected at wavelengths from 650 to 800 nm and from 560 to 650 nm, respectively. Bar = 10 μ m.

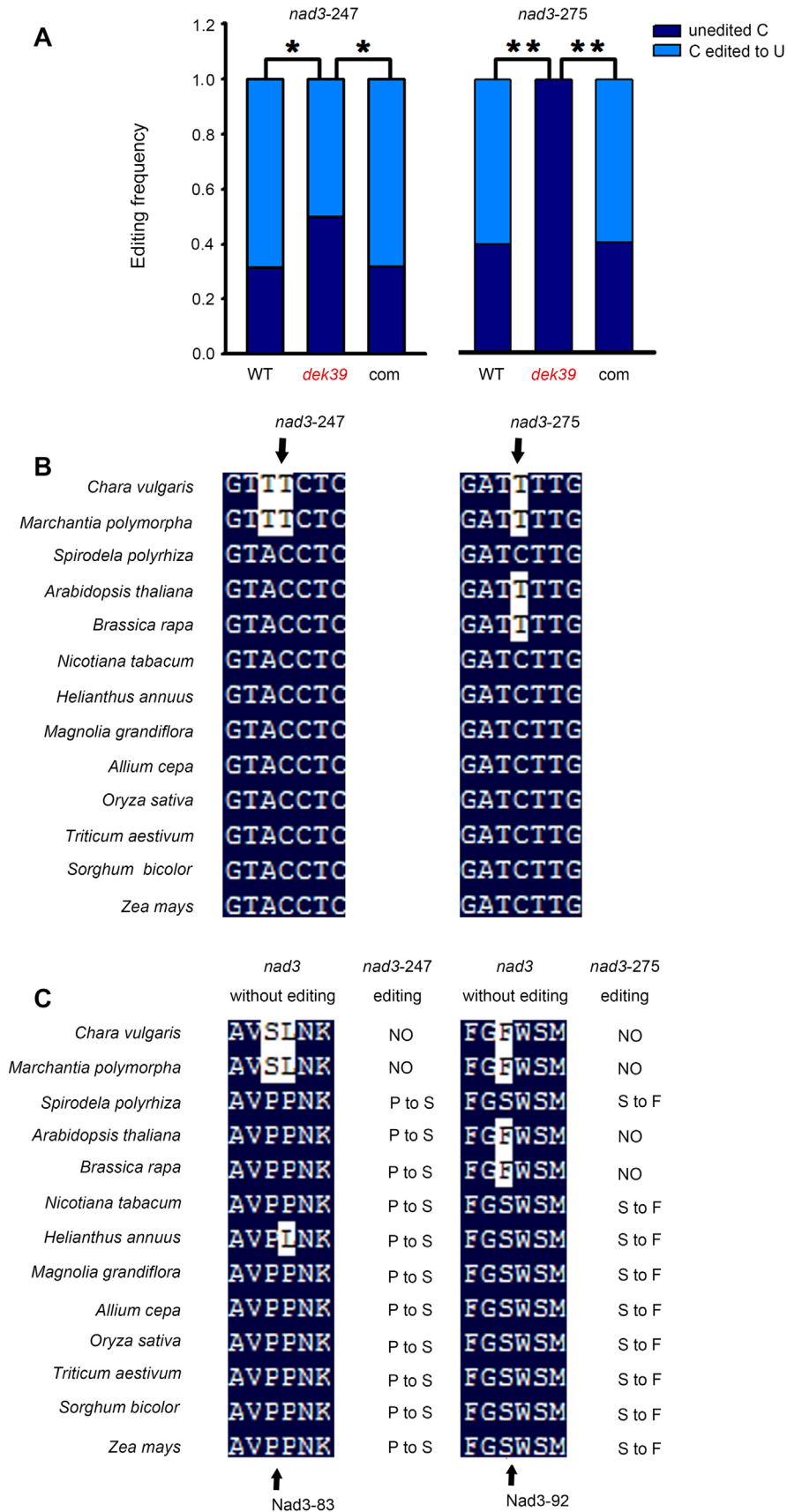


Figure 6. Continued.

Mitochondrial NADH dehydrogenase complex I activity in mutant *dek39*

Nad3 is one of the 14 core components of the mitochondrial NADH dehydrogenase complex (complex I). Complex I is the largest protein complex operating in oxidative phosphorylation and the major entry point for electrons from NADH entering into the respiratory chain. In maize, embryo lethality has been reported in defects of mitochondria caused by disruption of respiration.

To investigate whether the reductions of RNA editing at *nad3-247* and *nad3-275* affected the activity of complex I, mitochondria were isolated from 12 DAP kernels of mutant *dek39* and wild-type siblings, and protein complexes were separated by blue native polyacrylamide gel electrophoresis and subjected to an activity stain for NADH dehydrogenase (Figure 7). The identities of different complexes were determined based on their previously reported size in maize (Sosso et al. 2012; Li et al. 2014). The results revealed that no notable difference of abundance of complexes was observed between the wild-type and mutant (Figure 7A). However, the activity of complex I was reduced in *dek39* relative to that in the wild-type (Figure 7B). Three independent experiments of NADH dehydrogenase activity analysis were performed (Figure S4) and the results were quantitatively evaluated using the image J software (<https://imagej.nih.gov/ij/>, 1.6.0_24) (Sage and Unser 2003). The relative grey value of complex I activity was calculated by normalizing the grey value with DLDH. A statistical analysis showed that the activity of complex I in *dek39* was reduced to 66% of that in the wild-type and the reduction of NADH dehydrogenase activity was significant. The *P*-value was 0.02, less than 0.05 (Figure 7C). This result indicated that the reductions of editing at *nad3-247* and *nad3-275* decreased the activity of complex I in the mitochondrial electron transport chain without disrupting its assembly.

DISCUSSION

Dek39 is a dually targeting gene with a functional preference for mitochondria

Growing reports indicate that most PPR proteins function in organelles, with a few targeting the nucleus or cytoplasm (Colcombet et al. 2013). In *Arabidopsis*, not more than five PPR proteins are localized outside of the mitochondria or chloroplasts. These two organelles have many similarities in metabolic functions and many similar proteins can be found in both organelles. Some of these proteins are paralogs encoded by different genes, and the other proteins with identical sequence are translated from the same gene referred to as dual-targeting genes (Carrie and Small 2013). A systematic investigation of subcellular localization of 166 PPR proteins of *Arabidopsis* with ambiguous targeting predictions showed that dual targeting at both mitochondria and chloroplasts was more frequent than expected (Colcombet et al. 2013).

The requirements for mitochondria and chloroplasts are different in embryos and leaf cells, and it is impossible for all dual-targeted proteins to have equal distribution in mitochondria and chloroplasts. Dual-targeting genes have considerable implications for the control of their expression and function. Few dual-targeting PPR proteins are functionally characterized, and all of them show unequal need for the two organelles. *OTP87* encodes an E sub-class PPR protein and is required for RNA editing of the *nad7-24* and *atp1-1178* sites in *Arabidopsis* mitochondria. Experimental evidence shows that *OTP87* targets both mitochondria and chloroplasts, but *OTP87* is not essential for RNA editing in chloroplasts (Hammani et al. 2011). However, the ortholog of *OTP87* in rice *OsPPR1* was described to play a role in chloroplast biogenesis (Gothandam et al. 2005). *PPR2263* of maize and its *Arabidopsis* ortholog *MEF29* show dual localization with a preference for mitochondria, where they are involved in RNA editing of

← **Figure 6. RNA editing defects of *nad3-247* and *nad3-275* in mutant *dek39***

(A) RNA editing of *nad3-247* and *nad3-275* decreased in mutant *dek39*. WT, wild-type; com, complemented lines (one asterisk represents the significant difference, two asterisks represents highly significant difference). (B) Alignment of nucleotide around the *nad3-247* and *nad3-275* editing sites. (C) Alignment of amino acid sequences deduced from genomic DNA around the *nad3-247* and *nad3-275* sites. The amino acids in this region of Nad3 protein were less conserved between different plant species than other proteins encoded in mitochondria. Editing information was retrieved from the RNA editing Database (Picardi et al. 2007).

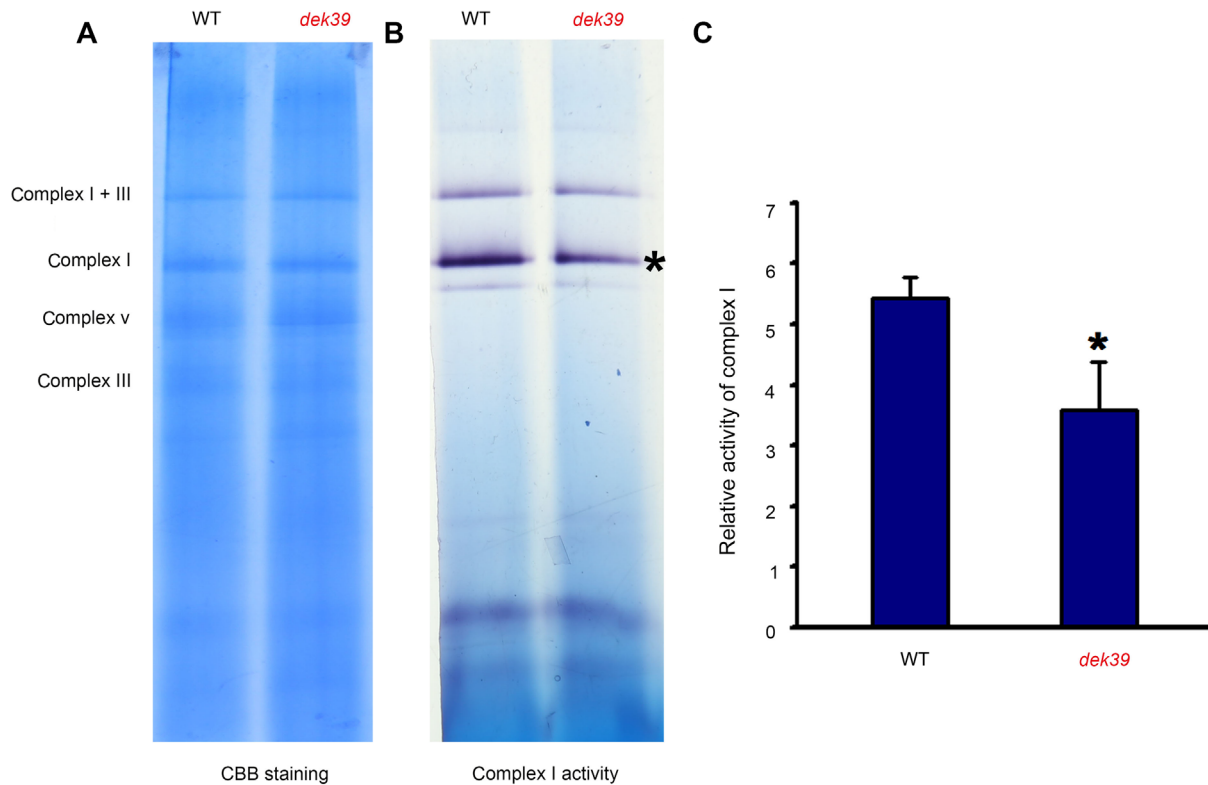


Figure 7. Protein gels of mitochondria isolated from wild-type and *dek39* endosperm at 12 DAP (days after pollination)

(A) Blue native (BN) gel stained with Coomassie blue. (B) NADH dehydrogenase activity of complex I. (C) The relative activity of complex I in WT and *dek39*. The asterisk indicates the significance of the reduction ($P = 0.02 < 0.05$ according to student's *t*-test). Mean values with standard errors of the mean were shown.

nad5 and *cob*, but their function remain ambiguous in plastids (Sosso et al. 2012).

DEK39 is a dual-targeting protein with a preference for mitochondria and is required for mitochondrial RNA editing of *nad3*, while RNA editing in plastids is not changed in *dek39*. DEK39 shows unequal function in these two organelles with a preference in mitochondria.

Editing of *nad3* is not conserved

Although most RNA editing events are located in protein coding regions and essential for correcting gene expressions, individual editing sites seem to disappear and reappear during evolution. Even between closely related species (Schmitz-Linneweber et al. 2005) or within species, such editing variation occurs (Tillich et al. 2005; Bentolila et al. 2008). In the mitochondrial genome, gene *rps12* harbors downstream of the *nad3* gene; these two genes are co-transcribed and the transcripts are edited at several sites, which are conserved in angiosperms (Pesole et al. 1996).

Investigation on *nad3-rps12* transcripts of sunflower, *Magnolia* and onion identified 26, 35 and 27 editing events, respectively (Perrotta et al. 1996). Editing of *nad3-rps12* is more extensive in *Magnolia*, and editing at *nad3-62* could be shown only in *Magnolia*, which is a species-specific codon modification. In addition, these plant species show marked variations in the degree of RNA editing, with only the *Magnolia nad3* being edited fully. Editing events of the two sites, *nad3-247* and *nad3-275*, where editing degrees are reduced in *dek39*, were identified in this investigation.

Variations of RNA editing are not only found in different plant species, or within the same species, but also during different development stages. After analyzing the C-to-U editing of *atp9*, *nad3*, and *cox2* in maize seedlings at various stages, they came to the conclusion that only *nad3* exhibits a different editing pattern while the cDNAs of *atp9* and *cox2* were completely edited. Incompletely edited cDNA of *nad3* was identified in all

tissues and an increasing editing degree was detected with growing seedlings, from 50% at 3 d to 75% at 7 d (Grosskopf and Mulligan 1996). Thus, the RNA editing status of *nad3* can change as the development and growth conditions change.

RNA editing in plants is very flexible and can be changed even more rapidly than the evolution of species. Concomitantly with the evolution of an editing site, the specificity conferring PPR proteins may be lost from the nuclear genome or be maintained depending on its requirement for editing at other target sites. MEF10 is required for RNA editing at *nad2-842* in mitochondria of *Arabidopsis*, but this editing site is already lost by its conversion to genomic T in *Beta vulgaris* and grape. Its ortholog in grape or *Beta vulgaris* is not required for this site and is likely to have shifted to a different site (Hartel et al. 2013). Editing at *nad3-275* has already been lost in *Arabidopsis*. In maize, DEK39 is required for the editing at *nad3-275* and its homolog in *Arabidopsis*, which is the most similar to DEK39, has accumulated so many amino acid differences in evolution that its actual targeting sites are likely shifted.

Lack of both editing sites reduces but does not eliminate the activity of complex I

Hatefi was the first to characterize the NADH dehydrogenase complex in bovine mitochondria (Hatefi et al. 1962). He subdivided the complex into four segments: the NADH dehydrogenase complex (complex I), the succinate dehydrogenase complex (complex II), the cytochrome c reductase complex (complex III), and the cytochrome c oxidase complex (complex IV) (Hatefi 1985).

Complex I is an L-shaped enzyme consisting of more than 40 components, including 14 conserved core subunits and 25 to 35 non-core subunits. All nine complex I Nad subunits (Nad1, 2, 3, 4, 4L, 5, 6, 7, and 9) are mitochondrial encoded (Subrahmanian et al. 2016). Abnormal transcription in *nad* genes lead to loss of complex I and impact assembly and activity of enzymes. Abolishment of *nad2* intron 4 splicing in *emp16* mutants (Xiu et al. 2016), reduced splicing efficiency in *nad4* intron 1 in *dek35* mutants (Chen et al. 2016) and incorrect splicing in *nad1* intron 1 in *dek2* mutants (Qi et al. 2017b) resulted in severe deficiency in complex I assembly and NADH dehydrogenase activity. Additionally, C-to-U editing at *nad* genes is critical to the function of complex I. Disrupted functions of complex I were

detected because of the lack of RNA editing at *nad7-836* (*smk1*) (Li et al. 2014), *nad3-250* (*slg1*) (Yuan and Liu 2012), *nad3-61*, and *nad3-62* (*dek10*) (Qi et al. 2017a). However, mutation in *Mef9* and *Mpr25* failed to edit site *nad7-200* and *nad5-1580*, respectively, which did not affect the NADH dehydrogenase activity of complex I (Takenaka 2010; Toda et al. 2012; Yap et al. 2015a). The loss of editing at these sites seemed to be tolerated.

Complete abolishment of complex I activity causes a severe growth phenotype (Li et al. 2014; Chen et al. 2016; Xiu et al. 2016). At the same time, several examples showed that significant decrease in the activity of complex I can also lead to severe growth or developmentally delayed phenotypes. RNA editing at *nad3-250* disappeared in mutant *slg1*, and the activity of complex I had significantly decreased but was not completely abolished. *slg1* plants exhibited slow growth and delayed development (Yuan and Liu 2012). Mutation in *Slo4* led to an editing defect in *nad4* and impaired the splicing efficiency of the first intron of *nad2*. In *slo4* knockout mutants of complex I was reduced to approximately 30% of that of the wild-type. These mutants displayed slow-growth phenotypes, and the *slo4* plants were much smaller than wild-type plants when grown on soil (Weissenberger et al. 2017). *mpr25* mutant seedlings exhibited a significantly shorter appearance than the wild-type seedlings. Editing of site *nad5-1580* was absent in *mpr25* but the NADH dehydrogenases activity of complex I was not affected. MPR25 protein was targeted to the mitochondria and may have been involved in the coordinated interaction between mitochondria and chloroplasts (Toda et al. 2012). Further research showed that the splicing of chloroplast *atpF* was affected in *mpr25* (Yap et al. 2015a), which might partially explain the growth deflection of *mpr25*.

PLS-PPR protein binding sites could span six to nine nucleotides upstream of the editing sites (Barkan et al. 2012). According to the PPR protein RNA recognition codes (Barkan et al. 2012; Takenaka et al. 2013; Cheng et al. 2016), 20 combinatorial codes for RNA nucleotides could be recognized by PPR repeats in DEK39, in which seven and eight nucleotides are present upstream of *nad3-247* and *nad3-275*, respectively (Figure S5). Our results showed that the editing efficiency of *nad3-247* was partially affected and the editing of *nad3-275* was completely abolished. This implies that the editing efficiency does not correlate with the number of

binding sites. Consistent with this view, it was recently found that six and nine nucleotides upstream of *ccmB-43* and *mrps4-335* could be recognized by PPR repeats of EMP9 and the editing efficiency of both sites in *emp9* was completely decreased (Yang et al. 2017).

Reduced editing at *nad3-247* and the lack of editing at *nad3-275* impacted the function of complex I. NADH dehydrogenase activity is decreased in *dek39*, but the reduced activity can still be detected, suggesting that unedited *nad3-275* seems to be partially tolerated. We speculate that energy produced in mutant *dek39* is not sufficient to maintain cell growth. When the energy level drops below a certain level, cell growth would stop, and the organism would die (De Block and Van Lijsebettens 2011). Therefore, *dek39* exhibits severe aberrant embryo/endosperm development and seedling growth. Although *Dek39* was a dual targeting gene in mitochondria and plastids, we did not detect a significant difference in RNA editing, RNA splicing and stability between the wild-type and *dek39* in plastids. We cannot exclude the possibility that *Dek39* edits RNA in plastids, which also contribute to the strong developmental phenotype in *dek39*, but the editing defects in plastids were beyond our detection. Further physiological and biochemical research of *dek39* will elucidate the function of *DEK39* in the plastid, which might provide more evidence to explain the severe seedling phenotype of *dek39*.

MATERIALS AND METHODS

Plant materials and culture

Mutant *dek39* was isolated from the mutant population induced by EMS mutagenesis in an inbred line B73 genetic background. The wild-type plants and kernels were either siblings of the mutant or B73. The mutation *dek39* was maintained in heterozygotes because of its lethal phenotype. The maize plants were grown in the experimental field at the China Agricultural University under the natural conditions. The transgenic lines were grown in a greenhouse with a 16 h/8 h light/dark cycle at 28°C/24°C without controlling relative humidity.

Light microscopy of cytological sections

Immature wild-type and *dek39* mutant kernels were collected from the same segregating ears of self-pollinated heterozygous plants at 12 DAP. The kernel

was cut along the longitudinal axis into three equal parts. The central slice containing the embryo was fixed at 4°C in 4% paraformaldehyde overnight. The fixed material was dehydrated in a graded ethanol series (50, 70, 80, 95, and 100% ethanol). After clearing with HistoChoice Clearing Agent (Sigma, H2779) and infiltrating with paraffin wax, the sample was embedded and sectioned at 8 µm with a Leica RM2235 slicer. The sections were stained with Hematoxylin and Eosin, and observed with Olympus SZ51 microscopy.

Map based cloning

As a first step of the mapping process, the heterozygous mutants were out-crossed with Mo17. Ears that were collected from self-pollinated F₁ generation exhibited segregating phenotype and miniature kernels were identified as homozygous mutants. DNA samples isolated from 30 individual miniature kernels were pooled, and confirmed the genotypes with 44 genetic markers, spaced approximately every 50 Mb apart on the ten chromosomes. Genetic linkage to three markers on chromosome 9 (9–50.1 Mb, 9–96.5 Mb, 9–149.7 Mb) was determined. Then another 300 small kernel samples were confirmed the genotypes with these three markers and a 53 Mb interval that contained the mutation were found. Additional markers were detected to narrow down the mutation region and finally approximately 9 Mb between markers 9–105 Mb and 9–114 Mb, which were used as flanking markers for fine mapping, the region had been determined. A population of 3,100 miniature kernels were analyzed with markers 9–105 Mb and 9–114 Mb and a total of 58 recombinants were identified. Additional markers in this region were used to find increasingly tight genetic linkage to the mutation. All the 58 recombinants were genotyped with these markers to narrow down the region of recombinant events and finally the mutation was fixed between 9–111.3 Mb and 9–112.5 Mb.

Genomic DNA was extracted from endosperms of small kernels which were segregated from F₂ generation using NaOH prior to keep at 99°C for 2 min. The PCR amplification was performed in 35 cycles with annealing temperatures between 58°C and 62°C and an extension time of 20 s. All the primers used in mapping are listed in Table S1. New markers were designed by comparing the sequence of B73 from the MaizeGDB and Mo17 from unpublished, high throughout sequencing data. The

mapping was carried out based on the protocol published before (Jander et al. 2002).

Complementation of *dek39*

The plasmid carrying *Dek39* promoter (−3,000 before “ATG”) and full-length *Dek39* cDNA fused MYC tag was constructed on the backbone of vector pCambia3100. *Agrobacterium*-mediated transformation of maize was performed following the published protocol (Zhu et al. 2016). First, we transformed the B73 to get positive transformation events and then crossed it with heterozygous (+/*dek39*) plants. Transgenic T1 plants were confirmed the genotype to identify heterozygote for the transgene *Dek39* and heterozygous mutation site for *dek39*. The double heterozygotes were self-pollinated to test whether the GRMZM2G345128 full-length DNA could genetically complement the *dek39* mutation.

Each transformation event was verified by PCR with primers DEK39-F and MYC-R. The complementation events used in phenotype analyses were also confirmed by Southern blotting. 50 µg DNA that extracted from the seedling at 14 d after sow was used for southern blotting. And we did Southern blotting according to the instruction of DIG High Prime DNA Labeling and Detection Starter Kit I (Roche).

Subcellular localization of DEK39

To generate a translational fusion between the DEK39 signal peptide and GFP, the full length open reading frame of *Dek39*, lacking its stop codon and *Dek39* (N417AA) fragment, was amplified by PCR with primers DEK39-F and DEK39-R/DEK39-417R on genomic DNA from maize inbred line B73 and introduced into the binary vector pCambia1300 by restriction enzymes and ligases. These binary constructs, which contained a 35S promoter driving constitutive expression of both DEK39-GFP and DEK39^{N417}-GFP, respectively, were transferred into *Agrobacterium tumefaciens* strain GV3101. The resulting strains were respectively co-infiltrated into *Nicotiana benthamiana* leaves with a strain harboring 35S:P19 (Li et al. 2012). GFP and MitoTracker red signals and chloroplast auto-fluorescence were detected by using of ZEISS LSM710 confocal microscopy at the wavelength of 560 to 650 nm and 650 to 800 nm respectively. The working concentration of MitoTracker was 100 nmol, and the samples were incubated at room temperature for 10 min.

RNA extraction and reverse transcription

Approximately 100 mg of fresh tissue was quickly frozen in liquid nitrogen and ground to powder with a mortar and a pestle. Total RNA was extracted with 1 mL Trizol reagent according to the instructions of the supplier (Invitrogen). After isopropanol precipitation, the RNA was re-suspended in 30 µL RNase-free water and treated with RNase-free DNase, which was then inactivated according to the manufacturer’s instructions. Approximately 4 µg of total RNA was reversely transcribed using Oligo (dT)₁₅ primer and M-MLV reverse transcriptase (Promega) with a final volume of 20 µL. Quantitative Real-time PCR analyses were performed using the SYBR *premix Ex Taq* kit (TaKaRa) according to the instruction of the supplier and the template provided as the following: 1 µL of a 10-fold dilution of cDNA in water in a total volume 20 µL. Real-time PCR for expression analysis of *Dek39* in maize organs was performed with primers DEK39-RT-F and DEK39-RT-R, which are listed in Table S1.

Analysis of mitochondria and plastids RNA editing

For RNA editing analysis in the wild-type and mutant *dek39*, total RNAs were extracted from endosperms at 12 DAP using the Trizol reagent according to the instructions of the supplier (Invitrogen). Total RNAs were treated with RiboMinus™ Plant Kit for RNA-Seq (Invitrogen A10838) to deplete ribosomal RNAs. RNA-seq libraries were prepared with the Illumina Standard mRNA-seq library preparation kit (Illumina) without poly-A selection and were sequenced to generate 101-nucleotide paired-end reads on an Illumina HiSeq platform. To check if the amount of data were adequate for the following analyses, data saturation analyses were performed here (Tarazona et al. 2015). We calculated the variation of gene numbers with increasing sequence depths. We calculated the Pearson correlation coefficient between two biological replicates with R software using genes expressed in the samples. Raw reads of the two biological replicates were first assembled by SOAPdenovo-Trans separately, and transcripts at the same locus were compared to identify the splicing sites (Xie et al. 2014). Raw reads were aligned to the mitochondrial and plastid genome using TopHat (Trapnell et al. 2009) and unique mapped reads were normalized as fragments per kilobase of exon per million fragments mapped (FPKM) to measure the transcript abundance. Each sample of the raw reads of two biological replicates were first merged, and

aligned to Maize B73 RefGen_V2 Mitochondrial genome with BWA-MEM(v0.7.5a) (Li 2014), SNP sites were called by Samtools(v1.3.1) (Li 2011). Editing frequencies of the same sites were calculated by Samtools mpileup.

To analyze the editing efficiency of *nad3-247* and *nad3-275*, mitochondrial cDNA was amplified and the PCR products were cloned into pMD-18. 57 and 67 independent clones from wild-type and *dek39* PCR products were respectively sequenced. Primers are listed in Table S1.

BN-PAGE and complex I in gel assay

Mitochondria of mutant *dek39* and wild-type sibling kernels at 12 DAP were isolated as previously described. The mitochondrial protein complexes were separated in BN-PAGE using Native-PAGE sample prep kits, according to the instructions of the supplier (Life Technologies). The in-gel complex I activity assay was performed as published (Li et al. 2014). We performed the NADH dehydrogenase activity three times. The bands were analyzed using the image J software (<https://imagej.nih.gov/ij/>, 1.6.0_24) (Sage and Unser 2003). The relative grey value of complex I activity was calculated by normalizing the grey value with DLDH. The *P*-value was required according to student's *t*-test.

ACKNOWLEDGEMENTS

This work was supported by the National Natural Science Foundation of China (91435206; 31421005), and National Key Technologies Research & Development Program-Seven Major Crops Breeding Project (2016YFD0101803, 2016YFD0100404), and the 948 project (2016-X33). These authors declare no conflict of interest.

AUTHOR CONTRIBUTIONS

X.L. and W.G. designed the experiments. X.L., W.G., S.S., Z.C., J.C., W.S. and H.Z. performed the experiments. X.L., W.G. and S.S. analyzed the data. X.L., W.G. and J.L. wrote the article.

REFERENCES

- Barkan A, Rojas M, Fujii S, Yap A, Chong YS, Bond CS, Small I (2012) A combinatorial amino acid code for RNA recognition by pentatricopeptide repeat proteins. **PLoS Genet** 8: e1002910
- Barkan A, Small I (2014) Pentatricopeptide repeat proteins in plants. **Annu Rev Plant Biol** 65: 415–442
- Bentolila S, Elliott LE, Hanson MR (2008) Genetic architecture of mitochondrial editing in *Arabidopsis thaliana*. **Genetics** 178: 1693–1708
- Bentolila S, Oh J, Hanson MR, Bukowski R (2013) Comprehensive high-resolution analysis of the role of an *Arabidopsis* gene family in RNA editing. **PLoS Genet** 9: e1003584
- Carrie C, Small I (2013) A reevaluation of dual-targeting of proteins to mitochondria and chloroplasts. **Biochim Biophys Acta** 1833: 253–259
- Chen J, Zeng B, Zhang M, Xie S, Wang G, Hauck A, Lai J (2014) Dynamic transcriptome landscape of maize embryo and endosperm development. **Plant Physiol** 166: 252–264
- Chen X, Feng F, Qi W, Xu L, Yao D, Wang Q, Song R (2016) Dek35 Encodes a PPR protein that affects cis-splicing of mitochondrial *nad4* intron 1 and seed development in maize. **Mol Plant** 10: 427–441
- Cheng S, Gutmann B, Zhong X, Ye Y, Fisher MF, Bai F, Castleden I, Song Y, Song B, Huang J, Liu X, Xu X, Lim BL, Bond CS, Yiu SM, Small I (2016) Redefining the structural motifs that determine RNA binding and RNA editing by pentatricopeptide repeat proteins in land plants. **Plant J** 85: 532–547
- Colcombet J, Lopez-Obando M, Heurtevin L, Bernard C, Martin K, Berthome R, Lurin C (2013) Systematic study of subcellular localization of *Arabidopsis* PPR proteins confirms a massive targeting to organelles. **RNA Biol** 10: 1557–1575
- De Block M, Van Lijsebettens M (2011) Energy efficiency and energy homeostasis as genetic and epigenetic components of plant performance and crop productivity. **Curr Opin Plant Biol** 14: 275–282
- Emanuelsson O, Nielsen H, Brunak S, von Heijne G (2000) Predicting subcellular localization of proteins based on their N-terminal amino acid sequence. **J Mol Biol** 300: 1005–1016
- Gothandam KM, Kim ES, Cho H, Chung YY (2005) OsPPR1, a pentatricopeptide repeat protein of rice is essential for the chloroplast biogenesis. **Plant Mol Biol** 58: 421–433
- Grosskopf D, Mulligan RM (1996) Developmental- and tissue-specificity of RNA editing in mitochondria of suspension-cultured maize cells and seedlings. **Curr Genet** 29: 556–563
- Hammani K, des Francs-Small CC, Takenaka M, Tanz SK, Okuda K, Shikanai T, Brennicke A, Small I (2011) The pentatricopeptide repeat protein OTP87 is essential for RNA editing of *nad7* and *atp1* transcripts in *Arabidopsis* mitochondria. **J Biol Chem** 286: 21361–21371
- Hammani K, Takenaka M, Miranda R, Barkan A (2016) A PPR protein in the PLS subfamily stabilizes the 5'-end of processed *rpl16* mRNAs in maize chloroplasts. **Nucleic Acids Res** 44: 4278–4288
- Hartel B, Zehrmann A, Verbitskiy D, van der Merwe JA, Brennicke A, Takenaka M (2013) MEF10 is required for RNA editing at *nad2-842* in mitochondria of *Arabidopsis thaliana* and interacts with MORF8. **Plant Mol Biol** 81: 337–346

- Hatefi Y (1985) The mitochondrial electron transport and oxidative phosphorylation system. **Annu Rev Biochem** 54: 1015–1069
- Hatefi Y, Haavik AG, Griffiths DE (1962) Studies on the electron transfer system. XL. Preparation and properties of mitochondrial DPNH-coenzyme Q reductase. **J Biol Chem** 237: 1676–1680
- Heazlewood JL, Howell KA, Millar AH (2003) Mitochondrial complex I from *Arabidopsis* and rice: Orthologs of mammalian and fungal components coupled with plant-specific subunits. **Biochim Biophys Acta** 1604: 159–169
- Hirose T, Sugiura M (1997) Both RNA editing and RNA cleavage are required for translation of tobacco chloroplast *ndhD* mRNA: A possible regulatory mechanism for the expression of a chloroplast operon consisting of functionally unrelated genes. **EMBO J** 16: 6804–6811
- Hirst J (2013) Mitochondrial complex I. **Annu Rev Biochem** 82: 551–575
- Hoch B, Maier RM, Appel K, Igloi GL, Kossel H (1991) Editing of a chloroplast mRNA by creation of an initiation codon. **Nature** 353: 178–180
- Jander G, Norris SR, Rounsley SD, Bush DF, Levin IM, Last RL (2002) *Arabidopsis* map-based cloning in the post-genome era. **Plant Physiol** 129: 440–450
- Kotera E, Tasaka M, Shikanai T (2005) A pentatricopeptide repeat protein is essential for RNA editing in chloroplasts. **Nature** 433: 326–330
- Li H (2011) A statistical framework for SNP calling, mutation discovery, association mapping and population genetical parameter estimation from sequencing data. **Bioinformatics** 27: 2987–2993
- Li H (2014) Toward better understanding of artifacts in variant calling from high-coverage samples. **Bioinformatics** 30: 2843–2851
- Li X, Qian W, Zhao Y, Wang C, Shen J, Zhu JK, Gong Z (2012) Antisilencing role of the RNA-directed DNA methylation pathway and a histone acetyltransferase in *Arabidopsis*. **Proc Natl Acad Sci USA** 109: 11425–11430
- Li XJ, Zhang YF, Hou M, Sun F, Shen Y, Xiu ZH, Wang X, Chen ZL, Sun SS, Small I, Tan BC (2014) *Small kernel 1* encodes a pentatricopeptide repeat protein required for mitochondrial *nad7* transcript editing and seed development in maize (*Zea mays*) and rice (*Oryza sativa*). **Plant J** 79: 797–809
- Liu YJ, Xiu ZH, Meeley R, Tan BC (2013) *Empty pericarp5* encodes a pentatricopeptide repeat protein that is required for mitochondrial RNA editing and seed development in maize. **Plant Cell** 25: 868–883
- Lurin C, Andres C, Aubourg S, Bellaoui M, Bitton F, Bruyere C, Caboche M, Debast C, Gualberto J, Hoffmann B, Lecharny A, Le Ret M, Martin-Magniette ML, Mireau H, Peeters N, Renou JP, Szurek B, Taconnat L, Small I (2004) Genome-wide analysis of *Arabidopsis* pentatricopeptide repeat proteins reveals their essential role in organelle biogenesis. **Plant Cell** 16: 2089–2103
- Maier RM, Hoch B, Zeltz P, Kossel H (1992) Internal editing of the maize chloroplast *ndhA* transcript restores codons for conserved amino acids. **Plant Cell** 4: 609–616
- O'Toole N, Hattori M, Andres C, Iida K, Lurin C, Schmitz-Linneweber C, Sugita M, Small I (2008) On the expansion of the pentatricopeptide repeat gene family in plants. **Mol Biol Evol** 25: 1120–1128
- Okuda K, Chateigner-Boutin AL, Nakamura T, Delannoy E, Sugita M, Myouga F, Motohashi R, Shinozaki K, Small I, Shikanai T (2009) Pentatricopeptide repeat proteins with the DYW motif have distinct molecular functions in RNA editing and RNA cleavage in *Arabidopsis* chloroplasts. **Plant Cell** 21: 146–156
- Perrotta G, Regina TM, Ceci LR, Quagliariello C (1996) Conservation of the organization of the mitochondrial *nad3* and *rps12* genes in evolutionarily distant angiosperms. **Mol Gen Genet** 251: 326–337
- Pesole G, Ceci LR, Gissi C, Saccone C, Quagliariello C (1996) Evolution of the *nad3-rps12* gene cluster in angiosperm mitochondria: Comparison of edited and unedited sequences. **J Mol Evol** 43: 447–452
- Picardi E, Regina TMR, Brennicke A, Quagliariello C (2007) REDIdb: The RNA editing database. **Nucleic Acids Res** 35: D173–D177
- Qi W, Tian Z, Lu L, Chen X, Chen X, Zhang W, Song R (2017a) Editing of mitochondrial transcripts *nad3* and *cox2* by Dek10 is essential for mitochondrial function and maize plant development. **Genetics** 205:1489–1501
- Qi W, Yang Y, Feng X, Zhang M, Song R (2017b) Mitochondrial function and maize kernel development requires Dek2, a pentatricopeptide repeat protein involved in *nad1* mRNA splicing. **Genetics** 205: 239–249
- Ruwe H, Castandet B, Schmitz-Linneweber C, Stern DB (2013) *Arabidopsis* chloroplast quantitative editotype. **FEBS Lett** 587: 1429–1433
- Sage D, Unser M (2003) Teaching image-processing programming in Java. **IEEE Signal Process. Mag.** pp. 43–52
- Schmitz-Linneweber C, Kushnir S, Babiychuk E, Poltnigg P, Herrmann RG, Maier RM (2005) Pigment deficiency in nightshade/tobacco hybrids is caused by the failure to edit the plastid ATPase alpha-subunit mRNA. **Plant Cell** 17: 1815–1828
- Schmitz-Linneweber C, Small I (2008) Pentatricopeptide repeat proteins: A socket set for organelle gene expression. **Trends Plant Sci** 13: 663–670
- Shikanai T (2015) RNA editing in plants: Machinery and flexibility of site recognition. **Biochim Biophys Acta** 1847: 779–785
- Sosso D, Mbalo S, Vernoud V, Gendrot G, Dedieu A, Chambrier P, Dauzat M, Heurtevin L, Guyon V, Takenaka M, Rogowsky PM (2012) PPR2263, a DYW-Subgroup Pentatricopeptide repeat protein, is required for mitochondrial *nad5* and *cob* transcript editing, mitochondrion biogenesis, and maize growth. **Plant Cell** 24: 676–691

- Subrahmanian N, Remacle C, Hamel PP (2016) Plant mitochondrial Complex I composition and assembly: A review. **Biochim Biophys Acta** 1857: 1001–1014
- Sun F, Wang X, Bonnard G, Shen Y, Xiu Z, Li X, Gao D, Zhang Z, Tan BC (2015) Empty pericarp7 encodes a mitochondrial E-subgroup pentatricopeptide repeat protein that is required for ccmFN editing, mitochondrial function and seed development in maize. **Plant J** 84: 283–295
- Takenaka M (2010) MEF9, an E-subclass pentatricopeptide repeat protein, is required for an RNA editing event in the *nad7* transcript in mitochondria of *Arabidopsis*. **Plant Physiol** 152: 939–947
- Takenaka M, Zehrmann A, Verbitskiy D, Hartel B, Brennicke A (2013) RNA editing in plants and its evolution. **Annu Rev Genet** 47: 335–352
- Tarazona S, Furio-Tari P, Turra D, Pietro AD, Nueda MJ, Ferrer A, Conesa A (2015) Data quality aware analysis of differential expression in RNA-seq with NOISeq R/Bioc package. **Nucleic Acids Res** 43: e140
- Tillich M, Funk HT, Schmitz-Linneweber C, Poltnigg P, Sabater B, Martin M, Maier RM (2005) Editing of plastid RNA in *Arabidopsis thaliana* ecotypes. **Plant J** 43: 708–715
- Toda T, Fujii S, Noguchi K, Kazama T, Toriyama K (2012) Rice MPR25 encodes a pentatricopeptide repeat protein and is essential for RNA editing of *nad5* transcripts in mitochondria. **Plant J** 72: 450–460
- Trapnell C, Pachter L, Salzberg SL (2009) TopHat: Discovering splice junctions with RNA-Seq. **Bioinformatics** 25: 1105–1111
- Wakasugi T, Hirose T, Horihata M, Tsudzuki T, Kossel H, Sugiura M (1996) Creation of a novel protein-coding region at the RNA level in black pine chloroplasts: The pattern of RNA editing in the gymnosperm chloroplast is different from that in angiosperms. **Proc Natl Acad Sci USA** 93: 8766–8770
- Weissenberger S, Soll J, Carrie C (2017) The PPR protein SLOW GROWTH 4 is involved in editing of *nad4* and affects the splicing of *nad2* intron 1. **Plant Mol Biol** 93: 355–368
- Wilson RK, Hanson MR (1996) Preferential RNA editing at specific sites within transcripts of two plant mitochondrial genes does not depend on transcriptional context or nuclear genotype. **Curr Genet** 30: 502–508
- Xia R, Wang J, Liu C, Wang Y, Wang Y, Zhai J, Liu J, Hong X, Cao X, Zhu JK, Gong Z (2006) ROR1/RPA2A, a putative replication protein A2, functions in epigenetic gene silencing and in regulation of meristem development in *Arabidopsis*. **Plant Cell** 18: 85–103
- Xie Y, Wu G, Tang J, Luo R, Patterson J, Liu S, Huang W, He G, Gu S, Li S, Zhou X, Lam TW, Li Y, Xu X, Wong GK, Wang J (2014) SOAPdenovo-Trans: De novo transcriptome assembly with short RNA-Seq reads. **Bioinformatics** 30: 1660–1666
- Xiu Z, Sun F, Shen Y, Zhang X, Jiang R, Bonnard G, Zhang J, Tan BC (2016) EMPTY PERICARP16 is required for mitochondrial *nad2* intron 4 cis-splicing, complex I assembly and seed development in maize. **Plant J** 85: 507–519
- Yang YZ, Ding S, Wang HC, Sun F, Huang WL, Song S, Xu C, Tan BC (2017) The pentatricopeptide repeat protein EMP9 is required for mitochondrial *ccmB* and *rps4* transcript editing, mitochondrial complex biogenesis and seed development in maize. **New Phytol** 214: 782–795
- Yap A, Kindgren P, Colas des Francs-Small C, Kazama T, Tanz SK, Toriyama K, Small I (2015a) AEF1/MPR25 is implicated in RNA editing of plastid *atpF* and mitochondrial *nad5*, and also promotes *atpF* splicing in *Arabidopsis* and rice. **Plant J** 81: 661–669
- Yap A, Kindgren P, des Francs-Small CC, Kazama T, Tanz SK, Toriyama K, Small I (2015b) AEF1/MPR25 is implicated in RNA editing of plastid *atpF* and mitochondrial *nad5*, and also promotes *atpF* splicing in *Arabidopsis* and rice. **Plant J** 81: 661–669
- Yuan H, Liu D (2012) Functional disruption of the pentatricopeptide protein SLG1 affects mitochondrial RNA editing, plant development, and responses to abiotic stresses in *Arabidopsis*. **Plant J** 70: 432–444
- Zehrmann A, van der Merwe JA, Verbitskiy D, Brennicke A, Takenaka M (2008) Seven large variations in the extent of RNA editing in plant mitochondria between three ecotypes of *Arabidopsis thaliana*. **Mitochondrion** 8: 319–327
- Zehrmann A, Verbitskiy D, van der Merwe JA, Brennicke A, Takenaka M (2009) A DYW domain-containing pentatricopeptide repeat protein is required for RNA editing at multiple sites in mitochondria of *Arabidopsis thaliana*. **Plant Cell** 21: 558–567
- Zhu J, Song N, Sun S, Yang W, Zhao H, Song W, Lai J (2016) Efficiency and inheritance of targeted mutagenesis in maize using CRISPR-Cas9. **J Genet Genomics** 43: 25–36

SUPPORTING INFORMATION

Additional Supporting Information may be found online in the supporting information tab for this article: <http://onlinelibrary.wiley.com/doi/10.1111/jipb.12602/supinfo>

Figure S1. Alignment of maize DEK39 protein with rice orthology *Oso6g0143500*, and the most similar protein *AT4G02750* in *Arabidopsis*

Figure S2. The data saturation analysis of the RNA-seq data

To illustrate whether the amount of the RNA-seq data was enough for our analysis, we did the data saturation analysis. With the increase of the sequencing depth, the curved line tended to be gentle. It indicated that the sequence data volume was enough for the analysis. **(A)** The data saturation analysis of RNA-seq data in mitochondria. **(B)** The data saturation analysis of RNA-seq data in chloroplast.

Figure S3. The correlation analysis between the replicates of the RNA-seq data in *dek39* and *wt*

(A) The correlation analysis in *dek39*. $R = 0.946$. (B) The correlation analysis in *wt*. $R = 0.938$.

Figure S4. NADH dehydrogenase activity of complex I
We tested NADH dehydrogenase activity of complex I for three times. Then we analyzed the activity through image J software quantitatively.

Figure S5. Alignment of the amino acid residues at position 6 and 1' in PPR repeats of DEK39 and RNA bases upstream of *nad3-247* and *nad3-275*

Nucleotides matching the recognition codes were shown in red color.

Table S1. Primers used in this work

Table S2. The coverage of the reads in the mitochondrial genes

Table S3. The coverage of the reads in the plastid genes

Table S4. Editing sites in transcripts of mitochondria

Table S5. Editing sites in transcripts of plastid



Scan using WeChat with your smartphone to view JIPB online



Scan with iPhone or iPad to view JIPB online